Test of Time Dilation Using Stored Li$^+$ Ions as Clocks at Relativistic Speed

Benjamin Botermann,[1] Dennis Bing,[2] Christopher Geppert,[1, 3, 4] Gerald Gwinner,[5] Theodor W. Hänsch,[6] Gerhard Huber,[7] Sergei Karpuk,[7] Andreas Krieger,[1] Thomas Kühl,[3] Wilfried Nörtershäuser,[1, 3, 8] Christian Novotny,[4] Sascha Reinhardt,[6] Rodolfo Sánchez,[4] Dirk Schwalm,[2] Thomas Stöhlker,[3] Andreas Wolf,[2] and Guido Saathoff[6]

[1]*Johannes Gutenberg-Universität Mainz, Institut für Kernchemie, 55128 Mainz, Germany*
[2]*Max-Planck-Institut für Kernphysik, 69117 Heidelberg, Germany*
[3]*GSI Helmholtzzentrum für Schwerionenforschung, 64291 Darmstadt, Germany*
[4]*Helmholtzinstitut Mainz, 55128 Mainz, Germany*
[5]*Department of Physics and Astronomy, University of Manitoba, Winnipeg, Manitoba R3T 2N2, Canada*
[6]*Max-Planck-Institut für Quantenoptik, 85748 Garching, Germany*
[7]*Johannes Gutenberg-Universität Mainz, Institut für Physik, 55128 Mainz, Germany*
[8]*TU Darmstadt, Institut für Kernphysik, 64289 Darmstadt, Germany*
(Dated: September 30, 2014)

We present the concluding result from an Ives-Stilwell-type time dilation experiment using ^{7}Li$^+$ ions confined at a velocity of $\beta = v/c = 0.338$ in the storage ring ESR at Darmstadt. A Λ-type three-level system within the hyperfine structure of the ^{7}Li$^+$ ^{3}S$_1 \to$ ^{3}P$_2$ line is driven by two laser beams aligned parallel and antiparallel relative to the ion beam. The lasers' Doppler shifted frequencies required for resonance are measured with an accuracy of $< 4 \times 10^{-9}$ using optical-optical double resonance spectroscopy. This allows us to verify the Special Relativity relation between the time dilation factor γ and the velocity β, $\gamma\sqrt{1-\beta^2} = 1$ to within $\pm 2.3 \times 10^{-9}$ at this velocity. The result, which is singled out by a high boost velocity β, is also interpreted within Lorentz Invariance violating test theories.

PACS numbers: 03.30.+p, 41.75.Ak, 42.62.Fi

With Special Relativity (SR), Local Lorentz Invariance (LI) has been established as one of the corner stones of all currently accepted theories describing nature on a fundamental level. Although empirically well established, the fundamental role of this space time symmetry in physics has accounted for incessant experimental tests with ever increasing scrutiny [1]. Interest in LI tests have been further boosted by the search for a theory reconciling quantum theory with general relativity, as many attempts for such a quantum gravity explicitly allow Lorentz violation [2–4], making it a potential discriminatory experimental signature for the underlying theory.

Within the wealth of Lorentz invariance tests, Ives-Stilwell (IS) experiments [5] stand out by using a large experimentally prepared Lorentz boost, which neither depends on sidereal variations nor on the assumption of any particular (*ad hoc* chosen) reference frame [6]. It directly verifies the time dilation factor γ, a salient consequence of Special Relativity (SR) of epistemological and technological relevance, via the relativistic Doppler formula: In SR the transition frequency ν_i of an atom at rest in an inertial system $\tilde{S}$, which is moving with a constant velocity $\beta = v/c$ in the laboratory system S, is related to the frequency ν measured by an observer at rest in S by

$$\nu_i = \nu\gamma(1 - \beta\cos\vartheta), \tag{1}$$

where ϑ is the observation angle with respect to the atom velocity β and $\gamma = 1/\sqrt{1-\beta^2}$. Ives and Stilwell were the first who actually showed the square root dependence of γ on $(1 - \beta^2)$ by measuring the wavelength of the H$_\beta$ line emitted parallel and antiparallel to hydrogen canal

rays [5]. We have implemented a modern version of this principle by driving two transitions ν_1 and ν_2 in a ^{7}Li$^+$ ion moving at velocity β with a copropagating (parallel) (p) and a counterpropagating (antiparallel) (a) laser beam. For resonance, the frequencies ν_p and ν_a of the two laser beams need to obey Eq. (1), which results in

$$\frac{\nu_a \nu_p}{\nu_1 \nu_2} = \frac{1}{\gamma^2(1-\beta^2)} = 1, \tag{2}$$

when compared to the corresponding rest-frame frequencies ν_1 and ν_2 measured in the laboratory system S. Note that the β independence of this relation and its contraction to one is not only a consequence of the special velocity dependence of the (kinematic) Lorentz factor γ governing time dilation but also relies on the validity of the relativity principle, namely that the atomic transition frequencies and the phase velocity of electromagnetic waves in vacuum are invariant under active (particle) Lorentz transformation.

Eq. (2) can be tested to high accuracy as it only depends on how precisely the four laboratory frequencies can be determined. While the boost velocity β cancels out and thus does not enter the error budget, the time dilation factor γ, however, increases to lowest order quadratically with β. Instead of quoting the IS observable

$$\epsilon(\beta) = \sqrt{\frac{\nu_a \nu_p}{\nu_1 \nu_2}} - 1 \tag{3}$$

it is therefore customary to use the reduced quantity $\alpha = \epsilon(\beta)/\beta^2$ when comparing different experiments aim-

ing at a validation of Eq. (2). Since the first experiment by Ives and Stilwell [5], which was performed at $\beta = 0.005$ and resulted in $|\alpha| \leq 10^{-2}$, several IS experiments have been performed with ever increasing sensitivity [7–11]. So far, the most accurate measurement employed saturation spectroscopy on $^7\text{Li}^+$ ions stored at $\beta = 0.03$ and $\beta = 0.064$ in the Heidelberg heavy ion storage ring (TSR) and resulted in $|\alpha| \leq 8.4 \times 10^{-8}$ [11].

The present Letter describes a measurement of ϵ employing optical-optical double resonance (OODR) spectroscopy on metastable $^7\text{Li}^+$ ions stored at relativistic velocities of 33.8%c in the experimental storage ring ESR of the GSI Helmholtzzentrum at Darmstadt. In a first version of this experiment [12], we showed the feasibility of OODR spectroscopy for an IS test under the harsh conditions of an accelerator laboratory. Here, we report on the analysis of an improved set of OODR measurements taking full account of their systematic uncertainties. As explained below, OODR on a Λ-type three-level transition yields higher signal-to-noise which is decisive for the present experiment as well as for sub-Doppler spectroscopy on thin ion beams in general. Also, OODR on an appropriate Λ transition with one transition frequency in the infrared might allow us to mitigate the strong Doppler blueshift keeping the necessary frequency for parallel excitation within the reach of narrowband lasers. This way, sub-Doppler spectroscopy might become feasible on ultrarelativistic beams of the upcoming FAIR facility.

The final result derived for ϵ, which constitutes the hitherto most sensitive model-independent validation of Eq. 2, will also be confronted with Lorentz-violating test theories. Because of its large Lorentz boost, our experiment might be especially sensitive to parameters of higher mass dimension in the Standard Model Extension test theory [13].

The $^3\text{S}_1 \rightarrow {}^3\text{P}_2$ transition of $^7\text{Li}^+$ is an appropriate clock for Doppler shift experiments. The metastable $^3\text{S}_1$ state lifetime of 50 s [14, 15] in vacuum, although reduced to $15 - 30$ s by collisions with residual gas atoms in the ESR, is still sufficiently long for spectroscopy. The transition wavelength of 548.5 nm is well within the optical region so that both parallel and antiparallel probe light can be generated by continuous wave lasers. The natural linewidth of 3.7 MHz is narrow enough to reach sub-MHz accuracy, the domain where systematic effects become dominant. And finally, Li ions can be accelerated and stored at high velocities and with excellent beam qualities.

The $^7\text{Li}^+$ ions are generated in a Penning ion gauge (PIG) source and accelerated by the GSI accelerator facility to a final energy of 58.6 MeV/u, which corresponds to a velocity of $\beta = 0.338$. The $^7\text{Li}^+$ ions are then transferred to the ESR where electron cooling [16] is employed to reduce the ion beam's longitudinal velocity spread to $\delta v/v \approx 9 \times 10^{-6}$ (FWHM) and its transverse diver-
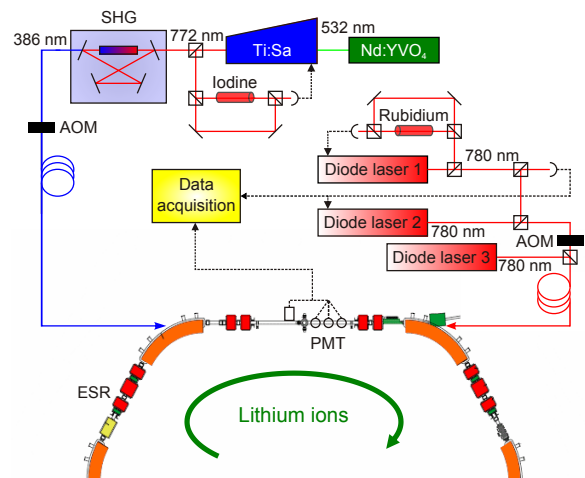

Figure 1: Left: Experimental setup. Laser system and data acquisition are inside a laser laboratory from which the light is guided to the ESR via polarization maintaining glass fibers.

gence in the experimental section to < 100 μrad. The metastable $^3\text{S}_1$ triplet ground state is weakly populated in the PIG source. After about 2 s of acceleration and injection and $7 - 20$ s of electron cooling, 10^7 to 10^8 ions are stored in the ESR with an estimated fraction of less than 1 % in the metastable $^3\text{S}_1$ state.

The $^7\text{Li}^+$ transitions are excited by lasers overlapping the ion beam parallel and antiparallel at Doppler-shifted wavelengths of 386 and 780 nm, respectively. Figure 1 shows the experimental setup. The light for parallel excitation at a fixed wavelength $\lambda_p = 386$ nm is generated by a titanium-sapphire (Ti:Sa) laser at 772 nm, pumped by a Nd:YVO$_4$ laser, and subsequent resonant second harmonic generation (SHG) in a beta barium borate crystal. The Ti:Sa laser is stabilized at 772 nm to the rovibronic P(42)1-14 transition in molecular $^{127}\text{I}_2$ by frequency modulation saturation spectroscopy [17]. This transition was calibrated versus a Rb clock using a frequency comb generator [18]. The light for antiparallel excitation, tunable around $\lambda_a = 780$ nm, is generated by a system of a low-power (20 mW, diode laser 1) and a high-power (58 mW, diode laser 2) external cavity diode laser, both in standard Littrow geometry. The low-power laser is fixed in frequency and referenced to a transition in ^{87}Rb [19] via frequency modulation saturation spectroscopy. The high-power laser is stabilized to the fixed-frequency laser via a tunable frequency-offset lock [20] allowing a tuning range of 600 MHz. The third laser diode running at $\lambda'_a = 780$ nm is controlled by a wave meter and used to increase the signal-to-noise ratio as discussed below.

After passing through acousto-optic frequency shifters (AOM), the light beams at λ_p and λ_a are guided together with that at λ'_a to the ESR via polarization maintaining fibers. The angles and positions of the laser beams are controlled with accuracies of $\Delta\vartheta = 20$ μrad

and $\Delta x = 50\,\mu$m by motorized rotation and translation stages. Overlap within $80\,\mu$rad between the laser beams and the ion beam is guaranteed with vertical and horizontal scrapers at two positions along the ESR experimental section. The fluorescence of the ions is detected by photomultipliers (PMT) in photon counting mode. Four types of spectra are taken applying (i) both lasers, (ii) λ_a only, (iii) λ_p only, and (iv) no laser. Using the AOMs, the lasers are switched between these four configurations in subsequent time windows of $100\,\mu$s duration, and the PMT signals are recorded in four different counters gated by the AOM switching signal. This scheme, which limits the measurement times per configuration to $\lesssim 100$ round-trips of the ions in the ESR, allows us to reduce background events as discussed below.

The remaining longitudinal velocity spread of the ^{7}Li$^+$ ions after electron cooling leads to Doppler broadening on the order of 1 GHz. To reach sub-MHz accuracy, we single out a narrow velocity class around a central velocity β_0 for the Doppler shift measurements. Simultaneous resonance of these ions with both lasers is probed to test Eq. (2). In our previous experiments at the TSR [10, 11], we employed saturation spectroscopy on the ^{3}S$_1(F = 5/2) \rightarrow \,^3P_2(F = 7/2)$ two-level transition and used the Lamb dip as the observable. At the ESR the number of metastable ions and, thus, the achievable signal-to-noise ratio turned out to be too small to apply saturation spectroscopy. We thus employed OODR spectroscopy on the Λ-type three-level system within the hyperfine structure of the ^{7}Li$^+$ ^{3}S$_1 \rightarrow \,^3$P$_2$ line to single out a narrow velocity class. Contrary to saturation spectroscopy where a small Lamb dip has to be identified within a large fluorescence background, OODR produces a positive peak on a small background and, thus, requires less scattered photons for a similar signal-to-noise ratio.

The Λ system used is composed of the ^{3}S$_1(F = 3/2) \rightarrow$ ^{3}P$_2(F = 5/2)$ and ^{3}S$_1(F = 5/2) \rightarrow \,^3P_2(F = 5/2)$ transitions with rest-frame frequencies ν_1 and ν_2, respectively. In the present experiment, the fixed-frequency parallel laser (λ_p) is resonant with the ^{3}S$_1(F = 3/2) \rightarrow$ ^{3}P$_2(F = 5/2)$ leg of the Λ for a central velocity class β_0 and pumps these ions into the ground state of the opposite leg. The second antiparallel laser (λ_a) is tuned across this opposite Λ leg. All ions, except those resonant with the fixed-frequency laser, are pumped dark after a few absorption and emission cycles. The Λ resonance appears due to the continuous back-and-forth pumping of the ions between the two ground states when the lasers resonantly drive both legs of the Λ for the same velocity class β_0.

Ideally, the linewidth of the Λ resonance should be mainly determined by the power-broadened and time-of-flight broadened natural linewidth. However, an ion circulating in the storage ring experiences velocity drifts within the Doppler distribution of the beam. Any group of ions pumped dark will, thus, get shifted back into res-
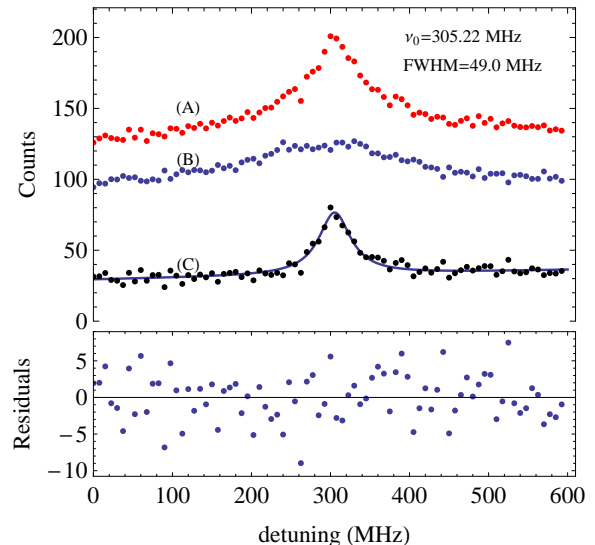

Figure 2: Typical fluorescence spectra obtained in an OODR run containing 44 laser scans. The scan direction is towards higher detuning. Upper graph: (A) Dark-count-rate reduced spectrum taken with all lasers on. (B) Spectrum obtained by summing the dark-count-rate reduced spectra taken with the parallel and antiparallel laser applied separately. Subtraction of spectrum (B) from (A) yields spectrum (C). The solid line reflects the fit of (C) by a Lorentzian together with a linear background. Lower graph: Residuals of the fit.

onance after many round-trips in the ESR. Depending on the velocity-drift dynamics and the frequency difference between the two laser beams in the ions' rest frame, these ions contribute background fluorescence and cause an additional broadening of the line shape. To reduce background contributions due to this drift-induced Λ fluorescence the switching scheme mentioned above was employed. Moreover, mainly caused by the laser-ion overlap in the ESR-bending magnets (see Fig. 1), the Λ system is not completely closed; to increase the signal-to-noise ratio, ions in the ^{3}S$_1(F = 1/2)$ hyperfine structure state are repumped into the Λ system by the antiparallel laser (λ_a'), which is tuned to the ^{3}S$_1(F = 1/2) \rightarrow \,^3P_2(F = 1/2)$ transition for ions at β_0.

Figure 2 shows a typical set of fluorescence spectra, where the PMT dark count rates determined in the measurement cycle (iv) have already been subtracted. The data are averaged over 44 laser scans. As the decay of the metastable ions causes a temporal decay of the fluorescence signal, we decoupled the scan from the ion injection cycle. After 69 of the 81 data points the laser scan is paused, new ions are injected and electron-cooled, and the laser scan is continued. Upon summing up many laser scans, the number of metastable ions contributing to each data point is approximately equal. Subtracting spectrum (B), which includes background caused by laser stray light and contributions from the drift-induced Λ flu-

orescence, from spectrum (A) taken with both lasers on simultaneously, one obtains spectrum (C), which displays the Λ resonance signal together with a smooth residual background. The fit of the residual spectrum (C) by a Lorentzian together with a linear background results in a central detuning frequency of $\nu_0 = 305.2$ MHz relative to the iodine marker and a linewidth (FWHM) of $\delta\nu_a = 49$ MHz. Transformed into the ^{7}Li$^+$ rest frame $\delta\nu_a$ results in a resonance width of 35 MHz, a factor of ~ 5 larger than expected from the natural line widths and the saturation as well as time-of-flight broadening. We believe that the major part of the resonance broadening as well as the residual background are caused by the drift-induced Λ fluorescence.

In total, we fitted 40 experimental Λ spectra with Lorentzians on a linear background. The fit residuals do not show any significant asymmetry or any other deviations from this model and we extracted a weighted average of the frequency ν_a of the antiparallel laser at resonance with a statistical uncertainty of 0.6 MHz. The slight asymmetry of the residual background and the influence of its approximation by a straight line on the frequency determination was simulated and is accounted for by a systematic uncertainty of 0.5 MHz. Table I summarizes the relevant frequencies and the uncertainty budget. Besides the statistical error, and the uncertainties caused by the residual background and the frequency stabilization of the laser diode, the dominant systematic uncertainty is due to the variation of the Gouy phases along

Table I: Frequencies with 1σ uncertainty budget used to determine ϵ by Eq. (3) (in MHz).

Rest frame frequencies	$\Delta\nu$
$\nu_1 = 546\ 455\ 143.0$ [21, 22]	0.43
$\nu_2 = 546\ 474\ 960.7$ [21, 22]	0.43
Doppler shifted frequencies	$\Delta\nu$
Antiparallel:	
$\quad$ Λ fit (weighted average of 40 spectra)	0.6
$\quad$ ^{87}Rb frequency reference	0.05
$\quad$ Frequency stabilization diode laser	0.64
$\quad$ Residual background linearization	0.5
$\quad$ Gouy phase shift	1.0
$\quad$ Angular laser and ion beam alignment	0.6
$\quad$ Ion beam divergence	0.4
$\nu_a = 384\ 225\ 534.98$	1.6
Parallel:	
$\quad$ ^{127}I$_2$ frequency reference	0.06
$\quad$ Frequency stabilization Ti:Sa	0.12
$\quad$ Gouy phase shift	1.0
$\quad$ Angular laser and ion beam alignment	0.6
$\quad$ Ion beam divergence	0.4
$\nu_p = 777\ 210\ 326.98$	1.25

the Gaussian laser beams. Ions moving along the laser beam direction experience this spatial phase variation as a frequency shift [11]. From an experimentally validated numerical simulation of this effect we infer a correction of $\nu_{\mathrm{Ph}} = 0.44 \pm 1.0$ MHz for each laser, using measured laser beam parameters. Further systematic uncertainties arise from the residual divergence of the electron-cooled ion beam as well as from a possible angular misalignment between laser and ion beams.

Inserting the rest-frame frequencies and the Doppler shifted frequencies into Eq. (3) we find

$$\epsilon(\beta) = \sqrt{\frac{\nu_a\nu_p}{\nu_1\nu_2}} - 1 = (1.5 \pm 2.3) \times 10^{-9}, \qquad (4)$$

at $\beta = 0.338$. From the experimental uncertainty, we find an upper limit for the reduced IS-observable of $|\alpha| = |\epsilon(\beta)/\beta^2| \leq 2.0 \times 10^{-8}$. This is not only a fourfold improvement over previous IS experiments [11], but in contrast to Ref. [11], where the measurement of the rest frequency was replaced by a measurement at low ion velocity assuming a polynomial dependence up to second order for $\epsilon(\beta)$, the present result is also independent of any assumption about the velocity dependence of $\epsilon(\beta)$.

When interpreted within the kinematic Robertson-Mansouri-Sexl (RMS) test theory [23–26], the IS experiment, together with the Michelson-Morley [27] and the Kennedy-Thorndike [28] experiments, belongs to the three classic tests of SR and the reduced observable α coincides with the RMS parameter $\hat{\alpha}^{(\mathrm{RMS})}$ [12]. In this model, $\hat{\alpha}^{(\mathrm{RMS})}$ is also accessible by experiments testing the anisotropy of the speed of light. The most accurate test of this kind used macroscopic clocks of the global positioning system and found a limit $|\hat{\alpha}^{(\mathrm{RMS})}| < 1 \times 10^{-6}$ [29], 50 times less sensitive than our experiment.

A dynamical test framework allowing for particle LI violations is provided by the Standard Model Extension (SME) [2, 30]. It is an effective field theory that extends the Standard Model Lagrangian density by Lorentz violating terms containing operators of arbitrary mass dimension. Within the hitherto worked out minimal SME, which is restricted to mass dimension ≤ 4, the IS experiment provides absolute bounds on proton and electron parameters [31, 32] as well as on the isotropy parameter in the photon sector [33] at a boost velocity of 0.34 c. We find $|\tilde{c}_Q^p| < 2 \times 10^{-11}$ for the proton and $|\tilde{c}_Q^e| < 2 \times 10^{-8}$ for the electron [34], both by many orders of magnitude less sensitive than Cs fountain clock [35] and microwave resonator [36] experiments, respectively, which, however, measure at velocities connected with sidereal variations. In the photon sector of the minimal SME we find a constraint for the isotropy parameter of $|\tilde{\kappa}_{tr}| \leq 2 \times 10^{-8}$. This is a factor of 20 short of the best direct test [37]. Other model-dependent constraints of these model parameters come from various experiments on high-energy cosmic rays [38] (10^{-20} level), relativis-

tic electrons [39, 40], and contributions to the anomalous magnetic moment of the electron [41].

As several systematic uncertainties are in the same order of magnitude and each of them difficult to improve, the constraint of Eq. (4) constitutes the concluding result of a generation of storage-ring based Ives-Stilwell experiments. While its sensitivity to the minimal SME parameters is lower than those of astrophysical observations and interferometer experiments, both searching for sidereal variations, the IS experiment stands out as one of the few absolute measurements being independent from sidereal variations by using an experimentally prepared large Lorentz boost. For a putative effect that scales with β^4, our result sets a 100-fold stronger limit than previous measurements [8, 11, 12]. The full benefit of this boost may only become visible when analyzed in the full SME including operators of higher mass dimension. This challenging theoretical work has only begun [13].

[1] D. Mattingly, Living Rev. Relativity **8**, 5 (2005); *Proceedings of the Fifth Meeting on CPT and Lorentz Symmetry, Bloomington, USA, 28 June - 2 July 2010,* edited by V.A. Kostelecký (World Scientific, Singapore, 2010).

[2] V.A. Kostelecký, and S. Samuel, Phys. Rev. D **39**, 683 (1989).

[3] G. Amelino-Camelia, Living Rev. Relativity **16**, 5 (2013).

[4] C. Rovelli, Living Rev. Relativity **11**, 5 (2008).

[5] H.E. Ives and G.R. Stilwell, J. Opt. Soc. Am. **28**, 215 (1938).

[6] G. Gwinner, Mod. Phys. Lett. A **20**,791 (2005).

[7] R.W. McGowan, D.M. Giltner, S.J. Sternberg, and S.A. Lee, Phys. Rev. Lett. **70**, 251 (1993).

[8] D.W. MacArthur *et al.*, Phys. Rev. Lett. **56**, 282 (1986).

[9] R. Grieser *et al.*, Appl. Phys. B **59**, 127 (1994).

[10] G. Saathoff *et al.*, Phys. Rev. Lett. **91**, 190403 (2003).

[11] S. Reinhardt *et al.*, Nat. Phys. **3**, 861 (2007).

[12] Ch. Novotny *et al.*, Phys. Rev. **A** 80, 022107 (2009).

[13] V. A. Kostelecký and M. Mewes, Phys. Rev. D **80**, 015020 (2009); Phys. Rev. D **88**, 096006 (2013).

[14] G.W.F. Drake, Phys. Rev. A **3**, 908 (1971).

[15] R.D. Knight and M. H. Prior, Phys. Rev. A **21**, 179 (1980).

[16] M. Steck *et al.*, Nucl. Instrum. Methods Phys. Res., Sec. A **532**, 357 (2004).

[17] J.L. Hall *et al.*, Appl. Phys. Lett. **39**, 680 (1981).

[18] S. Reinhardt *et al.*, Opt. Commun. **274**, 354 (2007).

[19] G.P. Barwood *et al.*, Appl. Phys. B **53**, 142 (1991).

[20] U. Schünemann *et al.*, Rev. Sci. Instrum. **70**, 242 (1999).

[21] E. Riis *et al.*, Phys. Rev. A **49**, 207 (1994).

[22] J. Kowalski *et al.*, Hyperfine Interact. 15/16 159 (1983).

[23] H.P. Robertson, Rev. Mod. Phys. **21**, 378 (1949).

[24] R. Mansouri and R. U. Sexl, Gen. Relativ. Gravit. **8**, 497 (1977); **8**, 515 (1977); **8**, 809 (1977).

[25] M. Kretzschmar, Z. Phys. A **342**, 463 (1992).

[26] C.M. Will, Phys. Rev. **D** 45, 403 (1992).

[27] A.A. Michelson and E.W. Morley, Am. J. Sci. **34**, 333 (1887); S. Herrmann *et al.*, Phys. Rev. D **80**, 105011 (2009).

[28] R.J. Kennedy and E.M. Thorndike, Phys. Rev. **42**, 400 (1932); M. E. Tobar, P. Wolf, S. Bize, G. Santarelli, and V. Flambaum, Phys. Rev. D **81**, 022003 (2010).

[29] P. Wolf and G. Petit, Phys. Rev. **A** 56, 4405 (1997).

[30] V.A. Kostelecký, and M. Mewes, Phys. Rev. D **66**, 056005 (2002).

[31] C.D. Lane, Phys. Rev. D **72**, 016005 (2005).

[32] V.A. Kostelecký, and N. Russell, Rev. Mod. Phys. **83**, 11 (2011).

[33] M.E. Tobar, P. Wolf, A. Fowler, and J.G. Hartnett, Phys. Rev. D **71**, 025004 (2005); M. Hohensee, A. Glenday, C.H. Li, M.E. Tobar, and P. Wolf, Phys. Rev. D **75**, 049902(E) (2007).

[34] Values quoted in [31] for the TSR experiments are by a factor of 10 too low.

[35] P. Wolf, F. Chapelet, S. Bize, A. Clairon, Phys. Rev. Lett. **96**, 060801 (2006).

[36] H. Müller, P.L. Stanwix, M.E. Tobar, E. Ivanov, P. Wolf, S. Herrmann, A. Senger, E. Kovalchuk, and A. Peters, Phys. Rev. Lett. **99**, 050401 (2007).

[37] F.N. Baynes, A.N. Luiten, and M.E. Tobar, Phys. Rev. D **84**, 081101 (2011); F.N. Baynes, M.E. Tobar, and A.N. Luiten, Phys. Rev. Lett. **108**, 260801 (2012).

[38] F. R. Klinkhamer and M. Risse, Phys. Rev. D **77**, 117901 (2008).

[39] B. Altschul, Phys. Rev. D **80**, 091901 (2009).

[40] M.A. Hohensee, R. Lehnert, D.F. Phillips, and R.L. Walsworth, Phys. Rev. D **80**, 036010 (2009).

[41] C.D. Carone, M. Sher, and M. Vanderhaeghen, Phys. Rev. D **74**, 077901 (2006).